

A Viable, Atomistic, Kinetic, Unified Aether Theory

by Harold Kyriazi

University of Pittsburgh School of Medicine, Dept. of Neurobiology, Pittsburgh, PA.

Address correspondence to: htk@pitt.edu

A purely mechanical, atomistic aether-based paradigm for our universe is proposed. The theory's hypothetical, indestructible corpuscles must be extremely hard, tiny, and fast, and constitute a dilute but highly energetic gas. They must also be capable of violating the second law of thermodynamics so as to produce dynamic structures out of chaos. Needle-like corpuscles, termed gyrons, with a high degree of orientation-stabilizing axial spin, are conjectured to be able to organize themselves throughout space into a fine 3-D matrix of toroidal vortices that constitutes the vacuum. These vortices, both to exist and to explain gravity, must continually eject longitudinally-oriented, greatly superluminal speed "gravitational gyrons" (GGs). According to the theory developed here, 1) matter consists of collections of right- and left-twisting, stronger versions of the vacuum vortices, and gravitates due to the smaller reactive cross-section and hence lower pressure of GGs ejected from other matter versus from the vacuum, 2) the large-scale organization of galaxies into walls and filaments is at least partly explained by the gravitational pressure differential transitioning from attractive to repulsive at very large distances, 3) the dynamic aspects of the vacuum and its interactions with matter may explain the measured constancy of the speed of light as well as various quantum mechanical phenomena, 4) the Big Bang is an illusion, with the redshift-distance relationship being due to a slow, progressive weakening of the matrix over cosmic time scales—and possibly a concomitant strengthening of matter vortices—owing to competition between vacuum and matter vortices for ideal spin-rate gyrons, and 5) the present cycle of the universe began with a Big Crystallization—of which the cosmic microwave background radiation is a remnant—and will end with a Big Dissolution, of all vortices. The theory is testable at both the cosmological and subatomic levels, by data fitting and 3-D animation simulations, respectively.

Introduction

Mechanical aether theories were abandoned in the early part of the 20th century for lack of a workable, specific theory (1). Conceptually occupying space today, instead of vortex atoms and a mechanical aether we have various wavefunctions and fields—most recently the Higgs field—of whose basic constitution the physics community remains operationally agnostic (2). Here physics meets one of philosophy's oldest questions: what could possibly lie at the base of existence?

Mankind's thoughts about this question have diverged along two lines: the materialist and the non-materialist. A prime example is the atomism vs. polytheism of ancient Greece (3, 4). More recently we have the supporters of a mechanical aether such as James Clerk Maxwell and Lord Kelvin, who not only tried to devise their own models of the aether, but enthusiastically explored the mechanical, "shadow gravity" theory of Georges-Louis Le Sage, vs. those like Einstein who were willing to accept equation-obeying electromagnetic and gravitational fields as fundamental, i.e., irreducible (5, 6).

Materialists consider non-materialists to be purveyors of spiritualism, whose ideas are akin to Aristotle's "explanation" that rocks roll downhill and smoke rises because those are their proper places. Non-materialists, on the other hand, consider materialists to be naïve, asking "why should we assume that the very basis of existence will be just a miniature version of the macroscopic world of our experience?" Nevertheless, I consider it safe to say that almost everyone would favor an atomistic, kinetic, mechanical model, in which the primary objects of existence are the hard, indivisible "atomos" conceived by the ancient Greeks, and in which the vacuum and all known forces and forms of matter are explained by the motions and collisions of those corpuscles, over a purely descriptive, mathematical theory laden with sophism ("distant galaxies are not moving apart at faster than the speed of light – space is being created between them") and logical impossibility ("the vacuum is not nothing, but neither is it anything").

There seem to be two huge impediments to such a mechanical theory, however. Looming large is the 2nd law of thermodynamics, or law of increasing entropy. It seems to tell us that no gas of hard, colliding and recoiling particles can long maintain any structure, and after some time any closed system will end up with a random distribution of particle position and velocity. But the 2nd law is actually a purely empirical result that holds true for all the gas molecules we have dealt with, but for which no formal proof exists. All of its derivations are based on what Boltzmann termed "the assumption of molecular chaos" (7). A mechanistic rationale is herein presented for why it does not apply to the fundamental corpuscles postulated here.

The other major perceived impediment to any mechanical aether theory is the various experiments—such as those of Michelson and Morley—that led to the development of special relativity, and which many mistakenly consider to have ruled out the aether. However, Lorentz aether theory, in which a luminiferous aether is postulated to exist and in whose reference frame—and only in whose reference frame—light's speed is truly isotropic, is indistinguishable mathematically from special relativity, and is thus a perfectly valid point of view (8-10). It is less favored, at least partly, because under it the measured constancy of the speed of light must be explained mechanistically rather than taken as axiomatic of the behavior of "spacetime," and no satisfactory mechanical model has ever been proposed.

A longstanding, fundamental shortcoming of the standard model of particle physics has been its inability to incorporate gravity, and thus join general relativity with quantum mechanics. But a

“quantum mechanical” theory of gravity has existed since the time of Newton. The Fatio-Le Sage theory of “shadow gravity” (11-13) was revived in the 1870s by William Thomson/Lord Kelvin (14) and Samuel Tolver Preston (15, 16), and discussed at length by James Clerk Maxwell (17), but had its shortcomings (11-14, 17). The remedying of its flaws requires three additional things to be true, one of which—a highly energetic vacuum—modern cosmology and quantum mechanics have postulated and surmised, respectively, while the second—sub-nuclear-sized toroidal vortices existing everywhere and ejecting much smaller, fundamental corpuscles at greatly superluminal speed—helps provide a simple mechanical explanation for quantum non-locality. The third is the stipulation that at least some of those corpuscles are needle-like in shape, with enormous, orientation-stabilizing axial spin rates, and which seem capable of both violating the law of increasing entropy and providing a mechanism for stable vortices to exist. The theory also strongly predicts that gravity transitions to repulsive at large distances, which may help explain the large-scale structure of the universe.

Perhaps equally tellingly, in solving the mechanical gravity problem the theory arrives at the same type of structure for the luminiferous aether that physicists of the 19th century posited on the basis of optical and electromagnetic phenomena (18)—consisting of a matrix of tiny, highly energetic vortices—and for entirely different reasons. Whereas light-speed circulatory motion was required on a very small scale to explain the sideways nature of a magnetic field’s effect on a moving charge and the transverse nature and high speed of light waves, it is the linear, funneling aspect of a smoke ring type circulation, and its proposed ability to eject needle-like corpuscles longitudinally at ultra-light speed, that will here be shown to be vitally important for gravity.

A brief historical review is necessary, because the main focus here is the development of a mechanical theory of gravitation, and few aside from historians of physics have heard of Fatio-Le Sage gravity, also known as Le Sage gravity, shadow gravity, and push gravity. Toward that end the reader is directed to several sources (11, 13, 19). The best analyses and exposition the author has encountered, however, are available solely on-line, in the form of several essays on Kevin S. Brown’s MathPages website (12).

Shadow gravity

Nicholas Fatio de Duillier, a protégé of Newton, in 1690, and Georges-Louis Le Sage, in 1758, both postulated that tiny, greatly superluminal particles travel through space in all directions and collide occasionally with massive bodies, so that the latter cast faint shadows upon each other, establishing a pressure drop and net attraction between them. Le Sage termed these particles “ultramundane corpuscles” because he imagined them to come from beyond the reaches of our known world. The corpuscles’ high speed ($\gg c$) was necessary in order to avoid planetary orbital instability, the exceedingly rare interaction with matter was needed in order to explain gravity’s proportionality to mass rather than surface area, and an even rarer interaction with each other

was necessary in order to provide a long enough corpuscle mean free path to have gravity act over very great distances.

Both Fatio and Le Sage reasoned that the impacts with matter would have to be at least partially inelastic, else the corpuscles scattered from massive bodies would rebound with the same kinetic energy with which they approached, and the “reflected glow” from the shadowed regions of two bodies would cancel their shadows, negating any net attraction between them. Christiaan Huygens criticized Fatio’s theory, pointing out that because the corpuscles must rebound at a slower speed than they go in, they would accumulate (“condense”) around matter, eventually putting a stop to gravity. After three years of thought, Fatio realized that the problem could be resolved if the return flow rate were postulated to be arbitrarily close to that of an exceedingly fast inflow. By having the particles’ collisions with matter be almost totally elastic, and giving them an ultra-high initial speed (which they had to have anyway, for a different reason), they would rebound nearly as fast as they go in and still provide the required energy for gravity, the latter being proportional to the difference of the squares of the two speeds. This would minimize any “condensation” and noticeable reduction of gravitational strength over time.

In 1905, George Darwin, a son of Charles Darwin, showed that for bodies very close to one another, Le Sage gravity would display the $1/r^2$ relation only if the collisions between the corpuscles and matter were completely inelastic (20). Henri Poincaré used this result, in 1908, to elaborate upon a criticism first leveled by Maxwell (17), and showed that the earth would necessarily be absorbing, via ultramundane corpuscle bombardment, the equivalent of 10^{21} times the sun’s total energy output, which, it would seem, would quickly incinerate the planet (21). Moreover, based on lunar drag calculations, the corpuscles would have to move at least 10^{17} times c , in direct violation of the main postulate of special relativity.

Gyron Aether Theory (GAT)

Frank Meno

Beginning in 1991, in a series of articles (22-27) in a non-mainstream physics journal, and two later, self-published books (28, 29), Frank M. Meno (30) presented a novel, particle aether-based “Theory of Everything,” postulating a semi-concave, needle-like shape and Planck-length size for the aether particles, and providing a plausible toroidal vortex structure for the electron (and positron) that he claimed reproduces all of its electromagnetic properties. For the theory presented here, three ideas were taken from Meno: the gyron (its shape, length, and spatial concentration), the vortex, and the latter’s ejection of longitudinally-oriented gyrons at much greater than light speed. (His proposed, density gradient mechanism for gravity cannot work for a variety of reasons, and is not discussed here.)

Gyrons

Figure 1A shows the main structural features of the proposed fundamental particle, along with definitions of spin vs. twirl. Meno proposed it to be Planck length in length ($1.616 * 10^{-35}$ m), and that supposition, for lack of evidence to the contrary, is maintained here. (Meno also proposed their RMS speed to be c , but even its non-GG component is here conjectured to be up to an order of magnitude greater.) Its width is greatly exaggerated to reveal the pointy tips and that most of the volume (“mass”) is located on the ends; the view in 1B is much closer to what Meno envisioned, although still eight times wider at its “hips” and “shoulders” than he supposed.

The tips are postulated to be pointy so as to minimize head-on collisions of GGs, and the mass is amassed near the ends so as to provide maximal gyroscopic stabilization of orientation for rapidly spinning ones, which can, it is asserted, lead to self-grouping of like-oriented gyrons. The enlarged shoulders and hips also provide opportunity for z-axis momentum transfer as presumptive GGs are being accelerated within vortex funnels. Some rough calculations of average gyron kinetics are given in Section I of Supplementary Materials.

In calculations provided in Section II of Supplementary Materials, it is shown that the gyron width required to have individual, average GGs travel as many as 150 million light years without collision, given the high spatial density proposed by Meno ($10^{96}/\text{m}^3$) and assuming perfect GG alignment, is 47 orders of magnitude narrower than the 1:331 width-to-length ratio supposed by Meno. Even with that barely conceivable degree of skinniness, it should be noted that the angles at the hip and shoulder—especially at the “inner lip”—could still vary from nearly zero to 90 degrees or more.

The GGs’ greatly superluminal speed allows them to “run the gauntlet” successfully, i.e., if there is a collision, it is because the GG ran into another, relatively stationary, gyron; other gyrons generally do not run into them. Thus, a GG’s contact is generally on its face and only rarely elsewhere on its body.

It is here assumed that gyrons have infinitely smooth surfaces, infinitesimally short durations of contact, and infinitesimally small amounts of compression under collision, such that each one’s axial spin is eternal, and equipartition of energy operates only between translation and twirl, and not necessarily spin. But these simplifying assumptions may not be essential.

It is important to grasp the unusually dilute and highly energetic nature of this proposed gas. Were the gyrons of pencil length, each would have a cubic football field—including end zones—to itself. But they move so fast that, were their path unimpeded and their average speed equal to c and increased to match their pencil length, they would be able to traverse the width of the visible universe ($2 * 13.7$ billion light years) 10^{17} times each second. Simulations of such a gas will be computationally intensive.

Self-grouping behavior

The mutual collisional cross-section of high spin rate gyrons, hereafter referred to as “spinners,” is smallest for those of like orientation. Their orientation and degree of precession are changed very little under ordinary, c-speed collisions—and the change in orientation and degree of precession can be made arbitrarily small by supposing the spin rate to be appropriately large. Spinners that find themselves in the neighborhood of like-oriented ones will experience longer mean path lengths and lower collision rates, tending to drift past their like-oriented brethren, and subsequently to bounce back—into the “flock”—from cross-oriented ones (31). Such flocks of like-oriented spinners can be stable only in closed loop structures, owing to the essentially zero cross section along the z-axis. Most stable would be arrangements where each such flock is surrounded by cross-oriented ones, maximizing the “bounce back” phenomenon.

Vortex structure and dynamics

It is here simply asserted—but can be proven only through detailed 3-D animation simulations—that an initially random position and velocity distribution of spinners would evolve, *via* the above-described “drift-past-same-bounce-back-from-other” phenomenon, into a matrix of right- and left-twisted toroidal vortices. One such vortex is illustrated in Figure 2. Topologically, it consists of a thin, cylindrical flock that has been bent into a ring, with a cross-oriented, toroidally-shaped flock bordering and confining it on all sides. The spinners comprising the toroid—hereafter referred to as “vortex engine gyrons” (VEGs)—have their body axes aligned with the vortex axis as they pass through the funnel, and orbit by “surfing” a radial inflow (see 2nd paragraph below and arrows in Figure 2C) by one or both of the mechanisms illustrated in Figure 1C (see legend). Their northern ends continually lead, i.e., point outward from the vortex center and tilt in the direction of the orbit, which curves only slightly between their exit in the north and re-entrance into the southern pole. The curve continues in the same direction the whole way, like the self-looped slinky toy pictured in Figure 2C.

The main feature of the vortex from a gravity standpoint is its ejection of longitudinally-oriented, “stealth mode” gyrons at ultra-light speed—the GGs. The proposed mechanism for this enormous acceleration is the scissoring action illustrated in Figure 2E. It is important to realize that each vortex stands, in relation to the size of individual gyrons, in the same proportion as a small galaxy does to a human being. With such a relatively long vortex funnel to work with, it is not too difficult to imagine such acceleration. It is, however, difficult to conceive how such a natural process could produce the essentially perfect alignment (“tuning”) of a spinner GG’s body axis and translational direction necessary to reduce its cross-section so much that it could travel many light years without collision. (Moreover, the first collision of even a perfectly tuned spinner GG, on its face, will result in a much greater sideways trajectory than its face angle, greatly increasing its cross-section and leading rapidly to catastrophic cascade collision (see Figure 1G and section III of Supplementary Materials).) To bypass this difficulty, it is instead proposed that the far-travelling GGs consist largely of well-tuned packets of “twirlers” (gyrons with essentially no

axial spin; Figure 1F). Such packets could suffer glancing collisions and lose only a single gyron per collision, with the rest of the tightly-packed twirlers traveling on virtually unscathed. In this way, a significant proportion of GGs could indeed travel rectilinearly a distance of many light years. Individually travelling GGs could follow closely behind such a packet, with the packet acting as a pathfinder.

The VEG orbits rely on a net radial inflow of motion derived from collisions of GG spinners with surrounding vortex cores (the dense rings and fast and dense funnels), whose spatial volume thus is responsible for a disproportionately large number of primary collisions. The collided spinner GGs on average do not reach maximal cross-section until traveling one-half the matrix unit distance in zigzag fashion (Figure 1G). The most closely-spaced and impactful collisions thus tend to occur there, creating a net cascade of motion toward adjacent vortices. Thus, the vortices, rather than being destroyed by the high speed bombardment of GGs, execute “judo throws” on the spinner component of the GG omnidirectional flux, using their “opponents” momentum against them, so as jointly to maintain their structure. (In order to work, the number of radially inflowing gyrons must be much greater than the number of VEGs, such that the collided inflowing gyrons, which must, on average, move after collision in the wrong direction—opposite the orbit—would rarely encounter another VEG before encountering other inflowing gyrons and being reabsorbed in the flow.)

This means that each vortex’s structure depends on that of its nearest neighbors, as well as upon the ejection of spinner GGs in their direction from more distant surrounding space, making it an especially interesting question how such a matrix of vortices can evolve. Presumably the self-organizing tendency leads to a jumble of long, snaking, cross-oriented cylinders that eventually loop back on themselves to form a system of weak vortices that gradually pick up speed (as they accumulate VEGs) and eject GGs at progressively higher speeds in a self-reinforcing, positive feedback loop (and setting the universal matrix up for possible later, catastrophic dissolution).

Differential pressure gravity

In order to explain gravity, matter must consist of vortices that are somehow stronger—producing more perfectly tuned GGs—than those of the vacuum. (Presumably they do this by having more and/or more ideal spin rate spinners—see below.) In this way, the GG pressure coming from matter is less than that elsewhere in space, making (near) gravity attractive. Thus, gravity is due to the difference in outward GG pressure exerted by matter vortices vs. vacuum vortices (Figure 4A-E).

All previous objections to Le Sage gravity have thus been answered. The “ultramundane corpuscles” come not from outside our universe but from everywhere within it. Gravity does not weaken over time because the omnidirectional GG flux is continually regenerated. The GGs do not accumulate around matter—hence also gradually weakening gravity—because they are ejected from matter vortices the same way they are ejected from vacuum vortices, and a dynamic

balance is maintained. The earth is not incinerated by the constant, high-speed bombardment because even more energetic GGs are ejected than are absorbed.

Vortex (as well as planetary scale) energy balance is maintained by a net inflow of high twirling rate gyrons, which must themselves exit at the same rate they enter (with much less average twirling motion) in order to maintain numerical balance (Figure 2D). They may do this either by recoiling from the vortex after colliding, or else by getting caught up in the flow pattern and exiting the north pole at low (sub-GG) speed in longitudinal orientation. The latter would exacerbate what I term “the motorboat problem,” which is how to supply enough northward momentum to the ejected GGs to avoid having the entire vortex putter backwards. One possible “larger sail” solution to that problem is illustrated in Figure 2F, which shows how the surfing VEGs may naturally present a larger cross-section while in the southern hemisphere than when in the north, owing to the orienting effect of their passage through the narrow, highly constricting funnel before exiting in the north, combined with a net excess of precession angle-increasing collisions from the radially inflowing twirlers. Other possible solutions, not elaborated here, involve a “greater wind” coming from the south for each vortex.

Because material vortices must eject more, and more perfectly tuned, GGs than those of the vacuum, at some large distance, where vacuum-ejected GGs have largely all collided, many material vortex GGs will continue on, such that at this large distance gravity necessarily transitions from attractive to repulsive (see Figure 4A-E).

Presumably the material vortices are stronger than those of the vacuum by virtue of having crossed a threshold that acts in a positive feedback manner—possibly by reciprocal vortex-strengthening interactions with its near neighbor vortices—to maintain that contingent of ideal spin rate spinners as more-or-less permanent VEGs. That ideal mix leads to the vortex ejecting more and better aligned GGs, perhaps packaging and ejecting twirlers in packets much more efficiently than vacuum vortices. (These twirlers must arise from either the radial inflow or from collided twirler GGs, whose collisions with the funnel and ring, and subsequent short-range catastrophic cascades, might help these dense core structures maintain each other’s integrity within each individual vortex; see Figure 1E.)

“Dark matter” analog in GAT

GAT offers several possible natural mechanisms to explain the apparent missing mass suggested by galaxy rotation curves, including one that could underlie Milgrom’s “Modified Newtonian Dynamics” hypothesis (MOND) (32), but they are complicated. One set of mechanisms would alter the force of the gravitational pressure differential being applied to the aether, while a second would alter the inertia exhibited by the aether (and any matter it includes) in response to that force. Both sets of mechanism are set up by the gyron density gradient (of undetermined magnitude) that exists as a consequence of the gravitational flow toward mass (which carries along the matrix and matter vortices, as well as free spinners), and which is accompanied by the

requisite counterflow of low twirl-rate twirlers (see Figure 2D). One set of mechanisms depends upon there being a gradient in free spinner concentration, while the other depends simply upon the overall gyron density gradient.

Acting to dissipate the gyron density gradient is the mixing action of the matrix (from vortices everywhere taking spinners and twirlers alike into their funnels and spitting them out at various speeds). This high speed, relatively short-range mixing effect will henceforth be referred to as “vortex churning action,” and is somewhat arbitrarily distinguished from the vortex-generated GG streams that act over much longer distances (and produce gravity).

Gravitational “constant” changes

It is possible that vacuum vortices in low mass regions contain fewer and/or less ideally spinning VEGs as a result of the above-described gyron density gradient, and their space containing fewer free spinners. As such, they would be somewhat weaker, and emit less well-tuned GGs than their counterparts in high mass regions of space. This could result in greater inward pressure on galaxy matter. At the same time and for the same reason, matter vortices along the outskirts of galaxies may also be somewhat weaker if they, too, are somewhat deficient in VEGs. Such matter would be less attractive than what we measure here on earth, its vortices being more similar to those of the vacuum. Conversely, any stronger matter vortices near the centers of galaxies might be more attractive than what we measure here on earth, resulting in greater-than-expected pull toward those centers. All of these phenomena would have the effect of keeping galactic matter in place.

Importantly, even if such differences in matter do exist, they may not be noticeable with regard to spectral properties, because the lower frequency light emitted by weak matter, for example, would have been produced in weak vacuum regions, where the speed of light is correspondingly slower. The slower speed of transmission would combine with the lower emitting frequency to yield approximately normal wavelength. The converse situation would obtain for strong matter vortices in galaxy centers. There, the higher frequency emissions would tend to be masked by the greater-than-normal light speed, which would act to spread out the more closely-spaced waves. The essentially perfect cancellation of these effects—one originating in matter and the other in the vacuum—would suggest that the mechanisms governing matter’s spectral lines and the vacuum’s propagation of light are one and the same, and that matter and its surrounding vacuum vortices are similar both in strength and structure.

An additional caveat remains, however, which is that matter vortices could already be at their maximum strength everywhere, such that their strength does not increase even if they are presented with additional and/or better spinners to incorporate as VEGs. (They may already have an ideal contingent of VEGs, such that attempting to add more only interferes with their structure and function.) Or, their strength could plateau at some point along the mass density and spinner gradient, such that G changes in a highly nonlinear way along that axis.

Gravitational dynamic changes

If, due to the gradient in overall gyron density, the return counterflow of low-twirl rate twirlers in low-mass regions is disproportionately easier than in higher mass regions (such as here on earth), it would constitute a mechanism to underlie the MOND hypothesis, serving to reduce inertia in those low-mass regions. One can imagine, for example, that having a bit more average room between gyrons might result in a disproportionately greater distance that vortex-ejected twirlers travel, allowing more easy acceleration of the matrix toward regions of greater mass.

The great success of MOND would seem to favor the latter, dynamic, inertial effects of the total gyron density gradient, and to disfavor the former, possible G-altering effects of the free spinner gradient. So, perhaps the free spinner gradient simply is not big enough to make a difference, while the overall gyron density gradient is.

Electrons/positrons

Meno postulated that electrons and positrons consist of individual vortices, one left-twisting and the other right-twisting. For lack of a better idea, that position is here assumed to be correct, and the vortex structure of Figure 2 applies to these as well as to vacuum vortices. (Meno does not seem to have considered the possibility of the existence of vacuum vortices, as he posited the vacuum to consist solely of randomly oriented, randomly moving gyrons.)

Nucleons

Meno did not offer his own structures for nucleons, other than to say that they are probably combinations of electrons and positrons (pp. 142-3 of ref 28). Here it is suggested that the proton consists of a 3+2 arrangement of positrons and electrons: an equilateral triangle of positrons plus one electron centered above and one below the plane, for a net charge of plus one (Figure 3A-C). The mutual repulsion of the three positrons is counterbalanced by the attraction to the two, polar electrons, while the mutual repulsion of the two electrons is counterbalanced by their attraction to the three, planar positrons. The neutron has an extra electron (Figure 3D). Presumably these nucleons exhibit much greater mass than the linear combination of their 5 or 6 electrons and positrons owing to cooperative effects that result in numerically denser core funnels and rings, faster movement through the funnels, and the ejection of more and better tuned GGs, especially from the longer, central, dual-electron funnel.

Electrical attraction and repulsion are assumed to be pressure differences resulting from like vs. opposing VEG flow patterns, respectively, that normally are mediated somehow by the matrix. The dynamics of the flow patterns for the closely apposed vortices within nucleons and atomic nuclei are likely complicated, and until realistic computer simulations of vortices have been achieved, further conjecture seems unwise. For example, secondary effects resulting from the periodic changes in cross-section of destabilized GGs might play a role here (and also in atomic electron orbital structure).

It is unclear how these axially tri-symmetric structures relate to the three quarks thought to comprise nucleons. Arguing against this simple model is the fact that protons seem to be made of two different types of quark. It is possible, though, that asymmetry is introduced by the surrounding matrix. Also arguing against such an arrangement is the exact equality of positron and proton charge despite their proposed huge structural and gyron flow pattern dissimilarities, as well as the perfectly neutral charge of the neutron.

Nuclei and the strong nuclear force

With these nucleon structures, it is easy to construct atomic nuclei that minimize charge repulsion (Figure 3E, F) and obey the rule that 5- and 8-nucleon nuclei are unstable, as it is clear that 4- and 7-nucleon nuclei are axially symmetric (Figure 3G-K), with no good place to put additional nucleons. (I would not be presenting these structures were it not for this happy and unexpected circumstance.) Presumably the instability of 5- and 8-nucleon nuclei is due to difficulties in reconciling the non-close-packed geometry of the proposed nucleon structures with the (presumed) close-packing of the matrix. But adding two additional nucleons, rather than one, to these planar structures – one above and one below the plane – would obviously produce more symmetrical, hence more stable, structures (such as lithium-6 and beryllium-9).

The attractive component of the strong nuclear force may be explained by these largely neutral charge stackings combined with micro-gravitational shielding produced by the gyron-dense core regions of the nucleon particles, consisting of the especially dense funnel core of the dual electron axis, along with those of the positrons and all of the stationary rings. The shadows formed by these dense structures—and thus the strong nuclear force—grow much faster than $1/r^2$ as the separation gets small, owing to their non-infinitesimal size. The repulsive aspect of the strong nuclear force presumably is explained by the judo throw distance (Figure 1G), closer than which the vortices cannot exist.

Atomic structure

The various electron orbitals of atoms must, under GAT, reflect the combination of the interaction of nuclear and matrix geometries and possibly the periodic nature of cross-section change of slightly destabilized GGs (Figure 1D, E), which may extend out well beyond matrix unit distance.

Relativistic considerations

It is clear that general relativity is obeyed, in this theory, due to the fact that the matrix is itself affected by the differential GG pressure of gravity, so that light, being a wave in the matrix, is naturally affected as well. Presumably matter cannot move faster than c because c reflects the orbital speed of VEGs. More difficult to explain are the special relativistic effects of length contraction and time dilation. The vortices that constitute a chunk of matter presumably move as a wave through the matrix of vacuum vortices, with only the additional, ideal spin rate spinners

actually being displaced. But discovering how this may occur must await detailed computer modeling of vortices.

Quantum mechanical strangeness

Quantum nonlocality may find its explanation in long-range, reciprocal exchange of GG streams by vortex complexes that produce effects essentially instantaneously, with the GG streams moving at speeds $\geq 2 \cdot 10^{12}c$ (33). An example of such a complex would be an arrangement like the proposed proton structure of Figure 3A-C, where the GG stream ejected by the central, dual-electron core goes one way, and the aligned triplet streams from the surrounding positrons go the other way, coupled with a proton facing the same direction. But rather than actual matter, these could be “sub-virtual” structures that normally exist only transiently in the vacuum matrix, perhaps moderating phenomena such as “photon entanglement,” etc.

Cosmological considerations

“Tired vacuum” vs. “tired light” and “dark energy”

The Type Ia supernova data that have been interpreted as an accelerating spatial expansion (and which is produced by “dark energy”), along with the fact that the stars of more distant, older galaxies are of a different composition than those in nearer, younger ones, indicate that the universe is not in a steady state. The former, along with the redshift-distance relationship, can be explained by a gradual weakening of the matrix over cosmic time scales, presumably due to competition between matter vortices (34) and those of the vacuum for ideal spin rate spinners, with matter gradually winning *via* the same threshold dynamics responsible for the maintenance of the matter/vacuum vortex distinction. The redshift may be due to one of a number of phenomena, all working toward the same effect. That matter vortices are postulated to be getting stronger and/or more plentiful, while the vacuum gets weaker, means that the light emitted by stars long ago may have had lower frequencies and longer wavelengths (i.e., redshifted relative to current processes), and that the speed of light was certainly greater before, so that wavelengths long ago were greater even for the same frequencies of emission. (This may be thought of as a “tired vacuum” version of Fritz Zwicky’s “tired light” hypothesis (35).) A properly timed acceleration of the rate of change would produce the Type Ia supernova data.

“Big Crystallization” vs. Big Bang”

According to GAT, then, the supposed universal spatial expansion of the Big Bang theory is an illusion; galaxies are not, on average, getting further apart. The current cycle of the universe likely instead began with a Big Crystallization of all vortex structure, and will end catastrophically with a Big Dissolution as matter vortices grow in strength and/or number relative to the vacuum to the point where the vacuum vortices break down, due to the dropping below of some minimum threshold in some aspect of the omnidirectional GG flux. At that point, matter vortices would immediately begin to dissolve. Each Big Crystallization inevitably is

seeded unevenly, owing to the previous cycle's uneven distribution of matter, with its attendant areas of concentrated high axial spin rate spinners. That degree of concentration could vary widely, depending upon the length of “down time” between each Big Dissolution and Big Crystallization.

If that down time is very short, such that the matrix merely “winks” briefly out of existence—just long enough for matter vortices to dissolve somewhat and replenish the vacuum with spinners—then the amount of matter formed during the Big Crystallization might have been only somewhat reduced from what it was just prior to the Big Dissolution. And in that case, GAT may be able adequately to explain the current distribution of matter by the usual “near” gravitational clumping combined with the added effect of repulsive “far” gravity (see Figure 4C-E). But this seems unlikely, as it would seem to leave little room for the past 13+ billion years of gradual vacuum weakening and matter strengthening.

More likely, then, the down time was relatively large, which permitted more diffusion of ideal spinners away from those regions where matter existed, such that the amount of matter formed initially by the Big Crystallization was much less than it is now, and with a much sparser distribution. Figure 4F suggests how such a sparse state could conceivably, *via* matter formation *de novo*, have led to the current observed large-scale structure of the universe. Such synthesis could occur only if enough ideal free spinners could be concentrated in a small volume, so as to cross the matter/vacuum vortex threshold. Such spinners could either have already been in the void spaces at low concentration at the time of the Big Crystallization, or could arrive there later, as far-travelling spinner GGs ejected from matter come to rest (that were following a pathfinding twirler packet). Some amount could also come from matter-rich regions due to the vortex churning action operating against the gravitational current. However the ideal spinners get to the void spaces, once there, the gravitational push from the repulsive, far gravity of the distant matter would tend to concentrate them in the middle. There, the conditions needed to form matter are likely very different from what they are for us here on earth, and closer to what they were at the time of the Big Crystallization, which might allow for cold nucleosynthesis.

The cosmic microwave background radiation (CMBR) is a remnant of the most recent Big Crystallization, and may be a by-product of the inevitable “jiggling” in the formation of the vacuum matrix itself, with the occasional pockets of matter having only a modulatory effect. This could explain the million-fold excess of CMBR photons relative to protons. And other possible explanations exist.

Discussion

GAT is fundamentally simple, yet operationally complex. The dilute gas proposed here to fill an infinite universe is radically different from other gases. The ultra-skinny gyron shape and (assumed) permanent gyroscopic properties of its spinners cause it to form vortex structures, in direct violation of the 2nd law of thermodynamics. Those vortices produce ultra-fast, non-

diffusional transport, or “vortex-assisted diffusion,” throughout space in the form of GG travel (Figure 4A). These vortices not only survive the bombardment from that omnidirectional GG flux, but are continually sustained by it in their current form and characteristic matrix spacing. The mere existence of such a flux means that ordinary, passive diffusion does not operate for the gyron gas except possibly during the inter-cycle interval, when the flux is diminished or non-existent.

The matter/anti-matter imbalance, under GAT, is rendered more apparent than real, as what we term “matter” is actually an equal mixture of both. The only “imbalance” remaining is the existence of atoms with nuclei consisting solely of protons and neutrons surrounded by electron clouds rather than equal amounts of these plus atoms with nuclei consisting of anti-protons and anti-neutrons surrounded by clouds of positrons. GAT might explain this atom-level asymmetry by a seeding mechanism during the Big Crystallization involving triplet streams of spinner GGs generated by some island of rapidly recrystallized prototype nucleons, whose spinners would be spinning either CW or CCW, but not both. Alternatively, the asymmetry might have evolved over multiple cycles, given incomplete dissolution of matter vortices each cycle. But such speculations can wait.

A large hole in GAT is that electromagnetic forces have not been worked out even roughly. Presumably the same sort of explanatory dynamics that MacCullagh, Maxwell, Fitzgerald, Kelvin, and Larmor envisioned in their 19th century mechanical models of the aether (18) will arise naturally from detailed 3D computer simulations of the matrix and its interactions with matter. There is also the question of how toroidal vortices give rise to spherically symmetric electric fields.

Another problem with GAT is that, under it, the fact that the time calculated for the Big Bang, based on the observed Hubble constant, agrees roughly with the ages calculated for the oldest stars, must be considered merely coincidental. For, under GAT, there is no obvious relationship between the processes governing the rate of stellar evolution and the rate at which the vacuum has undergone its proposed slow, steady weakening. And, under GAT an entirely new theory of primordial nucleosynthesis—possibly operating at low temperature—must be devised. A complicating factor is that, because the nascent vortices and GG fluxes coming into existence at the time of the Big Crystallization were very different than they are now, the factors governing nucleosynthesis may have been very different then.

Testing the theory

The deduced, gradual lessening of c over cosmic time scales, thought to be at least partly responsible for the redshift-distance relationship, would amount to a yearly decrease of 22 mm traveled per second if it were the only factor involved, and thus might be detectable. Another potential test is that gravitational lensing effects would be expected to shift to concave at large angles due to gravity being repulsive far away, but such effects may be undetectably small.

The easiest testing of GAT may be with regard to the large scale distribution of matter, given that gravity transitioning to repulsive at large distances is a hard prediction, and such simulations can be conducted relatively easily by experts. Hopefully the currently perceived need for dark matter will disappear, once the MOND hypothesis rationale is factored in.

Regarding testing at the sub-sub-nuclear level, detailed 3D simulations of individual gyrons in the numbers proposed to occupy the volume of a proton ($\sim 2.8 * 10^{-45} \text{ m}^3$), for example $\sim 10^{51}$ —are prohibitive, but I would expect that the “drift-past-same-bounce-back-from-other” self-grouping phenomenon would cause any initially random arrangement (in a “wrap-around space”) of large numbers (perhaps as few as tens of thousands) of spinners with random positions and linear velocities gradually to undergo a measurable reduction in collision rate. It should also be possible to test, by 3D modeling, the proposed mechanisms of vortex stability and GG ejection.

Although not vital for the overall theory, the proposed electron-positron composite structures for the proton and neutron, and the derived structures for small nuclei illustrated in Figure 3H-K, are easily put to the test by modeling larger nuclei, and seeing if the resulting geometric constraints reproduce the various “magic” atomic numbers, i.e., relatively stable (and presumably structurally more symmetrical) nuclei with certain numbers of protons and neutrons.

GAT represents a conceptual breakthrough, and promises to explain many current mysteries, such as gravity, the structures of the various instantiations of matter, the matter/anti-matter imbalance and quantum mechanics, on up through the large-scale structure of the universe and the CMBR. It may even elucidate the probable, infinite history of the universe itself. Large-scale, detailed 3D simulations are required, however, for the theory to achieve mathematical rigor and permit adequate testing. GAT’s explanations of phenomena are thus now necessarily sketchy, but I have here tried to show that the overall sketch is reasonable and, at least to a first approximation, consistent with observation.

References and Notes

1. Albert Einstein, *Ether and the Theory of Relativity*, (an address delivered on May 5th, 1920 at the University of Leyden), translated by George Barker Jeffery and Wilfrid Perrett, from *Sidelights on Relativity*, pp 3-24 (Methuen, London, 1922). Available on-line at http://en.wikisource.org/wiki/Ether_and_the_Theory_of_Relativity. “Neither Maxwell nor his followers succeeded in elaborating a mechanical model for the ether which might furnish a satisfactory mechanical interpretation of Maxwell’s laws of the electro-magnetic field. The laws were clear and simple, the mechanical interpretations clumsy and contradictory.”

2. See, for example, the many and varied interpretations of quantum mechanics described here:
http://en.wikipedia.org/wiki/Interpretations_of_quantum_mechanics#Summary_of_common_interpretations_of_quantum_mechanics.
3. Democritus and Lucretius offered atomism as an antidote to the irrational fears of people petrified by belief in unseen, unpredictable spirits everywhere, controlling life's events.
4. The Greek philosopher Parmenides stated, "*Only that can exist which can also be thought.*" (I interpret this to mean that if one cannot picture a concept, the concept itself must be flawed.) Andrew G. Van Melson, *From Atomos to Atom: The History of the Concept Atom*, p. 14, (Duchesne University Press, Pittsburgh, PA, 1952).
5. David E. Rowe, "Einstein's Allies and Enemies: Debating Relativity in Germany, 1916-1920", pp. 231-280, in *Interactions: Mathematics, Physics and Philosophy, 1860-1930*, eds. V. F. Hendricks, K. F. Jorgensen, J. Lutzen and S. A. Pedersen (Springer, 2006).
6. "The Bad Nauheim Debate (1920)", available on-line at
http://en.wikisource.org/wiki/The_Bad_Nauheim_Debate.
7. L. Boltzmann, *Lectures on Gas Theory* (originally published in two parts in 1896 and 1898), trans. By Stephen G. Brush, (Univ. of California Press, Berkeley, 1964).
8. Hsu, Jong-Ping and Zhang, Yuan-Zhong, *Lorentz and Poincaré Invariance: 100 Years of Relativity*, Advanced Series on Theoretical Physical Science, volume 8 (World Scientific Publishing Co., New Jersey, 2001).
9. Herbert E. Ives, Revisions of the Lorentz Transformations, *Proc. Am. Phil. Soc.*, **95** (2):125-131 (1951).
10. S. J. Prokhovnik, *The Logic of Special Relativity* (Cambridge Univ. Press, 1967).
11. Wikipedia entry on "Le Sage's Theory of Gravitation."
12. Kevin S Brown's www.mathpages.com essays (see his "Combined List of Articles") entitled "*Nicolas Fatio and the Cause of Gravity*", "*Historical Assessments of the Fatio-Le Sage Theory*", "*Le Sage's Shadows*", "*Fatio, Le Sage, and the Camisards*," and "*Omni-Directional flux.*"
13. James Evans; Frans van Lunteren; M. Edwards, in *Pushing Gravity: New perspectives on Le Sage's theory of gravitation*, Matthew R. Edwards, ed. (Apeiron, Montreal, 2002).
14. Sir William Thomson, On the Ultramundane Corpuscles of Le Sage, *Phil. Mag.* S.4, vol. **45**(301), (May 1873).

15. S. Tolver Preston, On some dynamical conditions applicable to Le Sage's theory of gravitation, *Phil. Mag.*, fifth series **4**, 206-210 (part 1), and 364-375 (part 2), 1877.
16. S. Tolver Preston, *Physics of the Ether* (E.& F.N. Spon, London and New York, 1875).
17. James Clerk-Maxwell, "Atom" entry in Encyclopedia Britannica, 9th Edition, ~1878. Also available in *The Scientific Papers of James Clerk Maxwell*, ed. by W. D. Niven, Dover Publications, Inc., New York.
18. Sir Edmund T. Whittaker, *A History of the Theories of Aether and Electricity*, vol. 1 (first published 1910, reprinted 1973 by Humanities Press Inc.)
19. Samuel Aronson, The gravitational Theory of Georges-Louis Le Sage, *The Natural Philosopher* **3**, (Jan. 1964).
20. George H. Darwin, The Analogy between Lesage's Theory of Gravitation and the Repulsion of Light, *Proc. Royal Soc.* **76**: 387-410 (1905).
21. H. Poincaré (1908), La dynamique de l'électron, *Revue generale des sciences pures et appliquees* **19**: 386-402. English translation by Francis Maitland, in Poincaré, H., *Science and Method*, Dover Publications Inc., 1952.
22. Frank M. Meno, A Planck-Length Atomistic Model of Physical Reality, *Physics Essays* **4**(1):94-104 (1991).
23. Frank M. Meno, Electromagnetics as Fluid Mechanics, *Physics Essays* **7**(4):450 (1994).
24. Frank M. Meno, Photons, Electrons, and Gravitation as Aether Dynamics, *Physics Essays* **8**(2):245 (1995).
25. Frank M. Meno, The Photon as an Aether Wave and its Quantized Parameters, *Physics Essays* **10**(2):304 (1997).
26. Frank M. Meno, A Smaller Bang?, *Physics Essays* **11**(2):307 (1998).
27. Frank M. Meno, *The photon and its Dynamic Structure*, *Physics Essays* **11**(3):467 (1998).
28. Frank M. Meno, *Cats, Atoms, Gyrons, Aether, and the Universe: Something for Everyone*, Aetherpress (self-published, 2000).
29. Frank M. Meno, *What Keeps Us on the Ground? Gravitation Explained*, Aetherpress (self-published, 2002).
30. A native of Slovenia, Meno (born Franz Mesojedec, changed to Frank Mesojedu upon arrival in the U.S., and to Meno in 1961 upon becoming a U.S. citizen) received a B.S.

degree in physics in 1961 from Pittsburgh's then-named Carnegie Institute of Technology, obtained a Masters in Electrical Engineering in 1969 from the renamed Carnegie Mellon University, and a Ph.D. in Biomedical Engineering in 1971 from the same institution. Aside from four years in the mid-1960s working at Gulf Oil as a research physicist, he was employed until his retirement mostly as a research assistant professor in the University of Pittsburgh's School of Medicine, working in the development of medical imaging technology, and held nine patents. He died on September 6 of 2010.

31. Center-of-mass collisions will result in immediate bounce back, but cross-oriented spinners undergoing non-center of mass collisions do so as well, and with little change in orientation. For a demonstration in Blender, using their Bullet Physics engine, see here: https://dl.dropboxusercontent.com/u/20014870/blender_spinning%20cylinders%20colliding_demo.avi
32. Mordehai Milgrom, Does Dark Matter Really Exist? *Scientific American*, **287**, 42-52 (August 2002).
33. T. Van Flandern, The Speed of Gravity: What the Experiments Say, *Phys. Lett. A* **250**: 1-11 (1998).
34. Rather than the vortices of all matter, it may be just those in the central cores of black holes, or even supermassive black holes, whose increase in number and/or strength is responsible for the universe's cycling. (If redshift quantization is ever shown conclusively to exist, it might argue for this.) The unique environment present there, surrounded by large volumes of nuclear matter, may create a more regular GG flux that allows the vortices there to be stronger and more retentive of VEGs than ordinary matter (see dashed lines of Figure 4A).
35. Fritz Zwicky, On the Red Shift of Spectral Lines through Interstellar Space, *PNAS* **15** (10): 773-779 (1929).

Acknowledgments

The author wishes to acknowledge the following: the late Frank Meno, for 28 years of learning, friendship, and discussion; Ben Monreal, now of the University of California at Santa Barbara, beginning when he was a post-doctoral fellow at the Massachusetts Institute of Technology, for critical comments and discussion related to statistical mechanics, photons, quantum mechanics, and modern physics in general; and Eugene Butikov of St. Petersburg State University, St. Petersburg, Russia, for instructive discussions about rigid body rotation.

Figure 1.

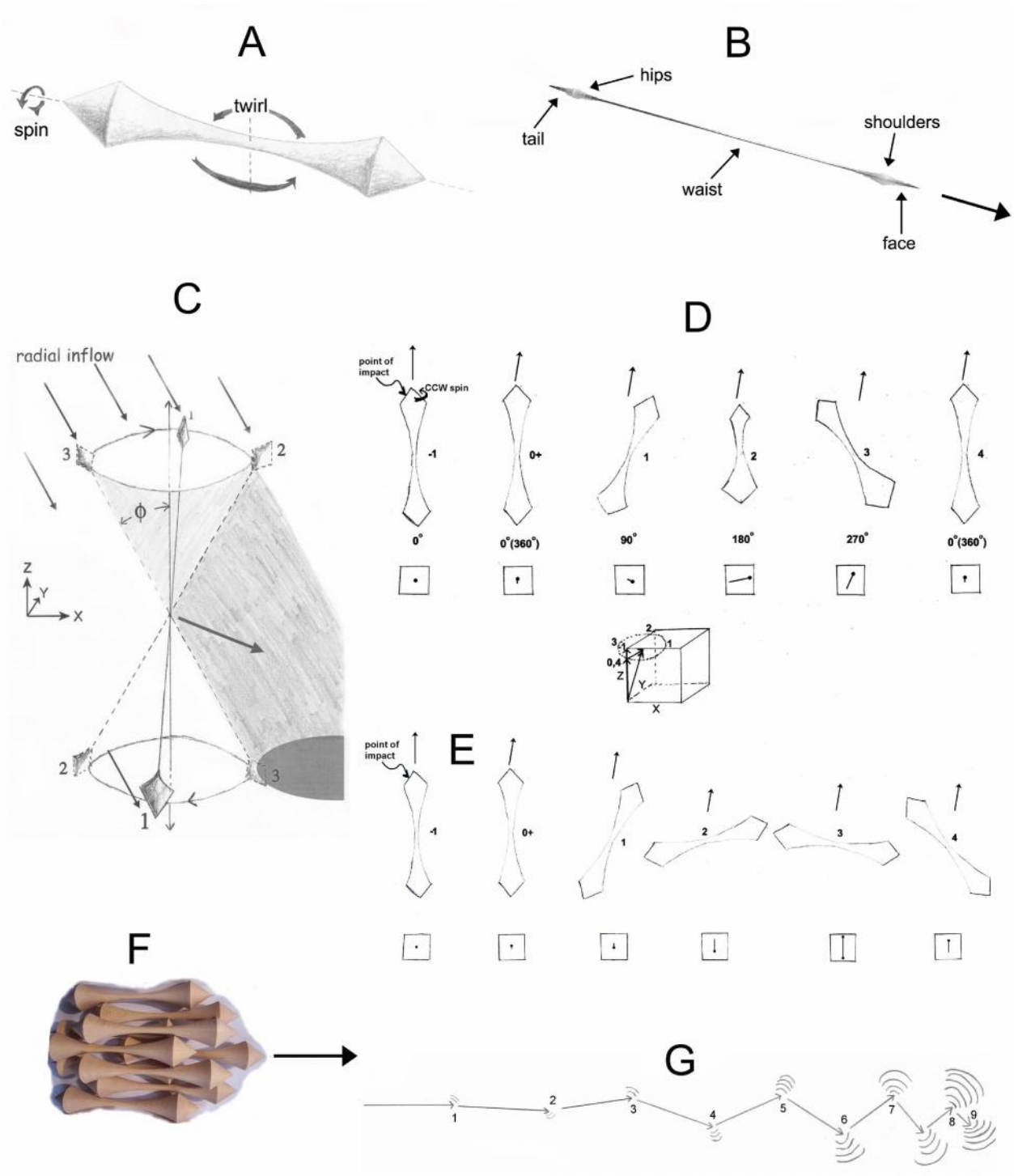


Fig. 1. Gyron shape and movement

A. Meno's postulated gyron shape, with width greatly exaggerated to illustrate the semi-concave shape throughout the middle ("waist") region (see part B). Pure "twirling" is the only form of rotation available for a gyron with no axial "spin." Conversely, gyrons with axial spin can never engage in pure twirling (i.e., "precessing" with a 90° angle). The end-heavy mass distribution contributes to spinner orientation stability under collision. The straight, conical tips allow for the least possible amount of deflection of gravitational gyrons (GGs) upon collision. The concave waist region may be postulated to form up to a 90° angle or more at the "inner lip" of the hip and shoulder (not shown), to allow more z-axis thrust to be provided to presumptive GGs in the vortex core by giving them a "handle" along their z-axes, especially during tight packing as in Part F.

B. A more proportionally correct gyron, with less exaggerated width, to emphasize both the overall thinness, and the thin waist (which is still twice Meno's suggested length:width ratio of 331:1). Here it is shown moving to the right, to allow labeling of a GG's head and tail regions. An ultra-thin waist region, combined with very sharp points at the tips (which may be essentially infinitesimal in size), would help make the probability of head-on, center-of-mass, tip-to-waist collisions between GGs and other gyrons vanishingly small, and glancing blows the norm for GGs.

C. Illustration of the mechanism(s) by which an engine gyron orbits its vortex by "surfing" the radial inflow (see Figure 2) as it precesses rapidly about its Z axis. Shoulder/hip width is greatly exaggerated to show orientation. The gyron is spinning clockwise along its length (as viewed from the top) and precessing in the same direction, as seen by its change of position from 1 to subsequent positions 2 and 3. Phi is the precession angle. The gyron is pointed, on average, in the Z direction, and spins along its own axis at a much greater rate than it precesses. The gyron moves mostly in the +X direction, with a bit of -Z as well, as indicated by the large arrow originating at its midsection. Two sources of asymmetry that lead to its proper orbit are illustrated. One is that its "inner half" (that on the far side of the radial inflow) is shaded from the inflow by the rapid precession of its outer half, such that collisions with inflowing gyrons tend to be on its outer half, and such as, on average, to not only thrust it in the +X direction, but cause a slight change in orientation in the direction of orbit. The second is the slightly greater torque exerted by hits on the outer tip than on the inner tip (see arrows next to each end of the gyron at position 1), due to the expanded shoulders and hips, which shields the tail region of the inner half.

D. "Destabilized" spinner GG precession. Time progresses from left to right. A GG with CCW axial spin is initially moving in the +Z (upward) direction. It impacts another gyron on the left side of its face region, which imparts some +X component to its linear motion, so that its final

trajectory (top arrows) has changing (and increasing) X and Z coordinate values (its center-of-mass Y coordinate remains at 0). The impact also induces some precession, which the cube at the bottom illustrates. It depicts the initial velocity vector along the Z axis (arrowhead by the “-1”), along with its now lesser z-axis vector (arrowhead next to “0,4”), which doubles as the initial angular momentum vector which, after impact, tilts into the plane of the paper (the non-vertical arrow in the y-z plane). The GG’s new cross-section then undergoes the periodic changes depicted in the squares. The lines inside the squares show the cross-section when viewed from the direction of the gyron’s current trajectory (top arrows). (NOTE: for the new trajectory, the view is one of looking down and facing to our left.) Dots indicate the tip of the gyron closest to the viewer. The now-destabilized GG will travel a few gyron lengths beyond the place where it was impacted before it displays its maximal cross-section (at 270°). That distance will vary depending on the gyron’s face angle and angular momentum. Only a face angle of the incredibly small amount of $\sim 10^{-15}$ of a degree would yield a distance approaching that of a reasonable matrix unit size of $> 10^{-20}$ m, and so the distance traveled during this precessional cross-section variation is likely important only in that it, along with that shown in E, would help maintain the spacing between the vortex core’s funnel and ring, which are separated by perhaps only a few Planck lengths. It, by itself, seems highly unlikely to be able to provide vortex inflows, except as one segment of a larger catastrophic cascade as shown in Part G.

E. Mechanics similar to D for a destabilized twirler GG. As mentioned in D, unless gyrons have incredibly gentle face angle slopes, these cyclic changes of cross-section would play no role except where gyrons are tightly packed – in the core’s funnel and ring. It may be that both these distances (in D and E) help determine the funnel-to-ring mutual spacing, while the main determinant of matrix unit size is illustrated in Part G.

F. Packet of twirler GGs. A rather poor illustration of a GG packet – poor both because of the small number of gyrons included, and because they are fat rather than ultra-skinny. Also, it may be possible to align them more like the front end of a Roman army “tortoise wedge,” which had densely arrayed shields protecting the interior against enemy spears and arrows. The two main features of the packet are its tight packing and streamlined, skinny toothpick, shape. Only rarely will a relatively stationary gyron collide with the packet in a totally disruptive way, by wedging its tip into the small gaps at the packet’s front. Most collisions will be somewhere along the packet’s outer envelope, and the impact will kick out the member of the packet on the opposite side (like an end billiard ball from a tight rack, or metal ball in a “Newton’s Cradle”), leaving the rest of the packet to continue on its trajectory undisturbed, although slowed slightly. This packet behavior will be vitally important for some of the ideas illustrated in Figure 4. The twirler kicked out of the packet would then behave essentially as in E.

G. “Judo throw,” zigzagging, catastrophic cascade trajectory of a destabilized spinner GG (such as shown in D). Note: the arrows represent the increasingly sideways trajectory of the spinner

GG, which itself remains essentially horizontal throughout, due to its high axial spin rate. Collisions at very shallow angles, such as those here labeled 1 and 2, are thought to occur many times, and their mean free paths are relatively much greater than illustrated here, whereas subsequent collisions, such as 5 through 9, have shorter mean free paths and relinquish much more of the GG's energy. The important thing is that spinner GGs will have cascade distances with roughly bell-shaped distributions, producing the "judo throw" distance that sets matrix unit size.

Figure 2.

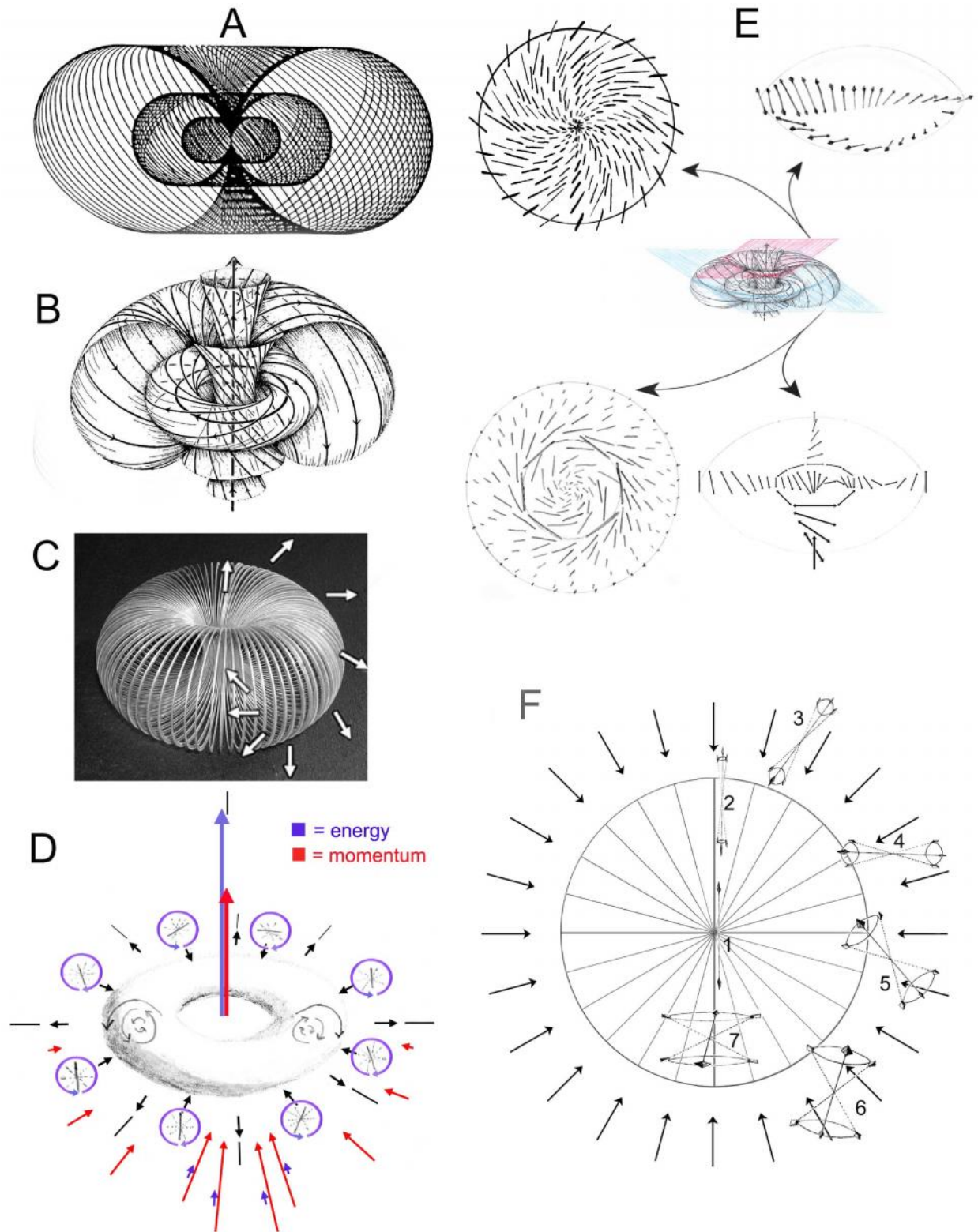


Fig. 2. Vortex structure and dynamics

A. Side cutaway view of the vortex, from ref. 24. The drawing misrepresents the situation, as it implies an infinite concentration of upward moving gyrons at the absolute center, while at any non-zero distance away from the center the flow is downward. More accurate is the drawing shown in part B.

B. A modified “Penrose twistor” (an entity whose etiology is not relevant here), better illustrating the vortex central core’s funnel and ring. Gyrons flow in a twisted smoke-ring fashion, as shown by the arrows. In the southern hemisphere, however, the flow in a twistor changes direction, which is not feasible for the orbiting, vortex engine gyrons (VEGs).

C. The proper flow pattern of VEGs illustrated by a slinky looped into a circle. The arrows indicate the orientation of a VEG orbiting to the right side. When viewed from the outside, the VEGs of this vortex constantly “surf” the radial inflow with a slight clockwise twist. To have the VEGs enter the south pole, the radial inflow must be augmented with a slight outward push, either from residual flow of VEGs coming from the opposite side, or from the off Z-axis spread of “almost-GGs” coming from a similarly oriented vortex situated directly below. (Vacuum vortices may form long, snaking, north-to-south oriented chains.)

D. Schematic illustration of the net energy, momentum, and gyron number balance of the vortex. Energy (a scalar quantity) is shown in blue, momentum (a vector) in red. There is a net inflow of fast twirlers (inside the blue circles) and equal outflow of slow twirlers (shown as lines), both shown only along the equator, but the former actually occurs in almost all directions. The inflowing twirlers constitute the radial inflow, and twirl randomly in all orientations (illustrated by the alternating CW and CCW direction of the circular blue arrows). Most of the energy of the ejected GGs (single line exiting at the top of the panel) comes from conversion of the twirling energy of the radial inflow, and very little from the south-to-north gyron motion entering the south pole. This conversion occurs via a mechanism illustrated in panel E. In contrast to energy, all of the momentum of the vastly ultra-light-speed ejected GGs (upward, central red arrow) must come from an excess of collisions of VEGs with south-to-north moving gyrons, which may arise from one or more mechanisms (see text, and Part F). In C, D, E and F, individual gyrons are drawn much bigger than to scale, so that the role of their orientation can be grasped.

E. Highly schematic cutaways of two different sections through a clockwise twisting vortex, with top and side-top views. The top cutaways (red slice) are above the equator, and the bottom ones (blue slice) are at the equator. The top views, at the left, show the “scissoring” action that produces the upward thrust of the core’s successive “inner tubes” in the southern hemisphere

(not shown). This scissoring mechanism derives from the radial inflow operating on the VEGs, which tend to be oriented, in the funnel, with their northern tips pointed outward and upward, similar to the way the same radial inflow causes them to orbit properly when they are outside the funnel (see arrows in Figure 2C, and orbiting gyron in Figure 2F). The scissoring action in the north is thought to provide continued fine-tuning of GG alignment. The side-top views, at the right, show the asymmetry of the front and center-line gyron cross-sections approaching (right side) and receding from (left side) the viewer. There is no significance to the number of gyron orientations drawn on the sides, front, and back. The lower panels illustrate an important point, that the toroid's ring consists of a dense packing of \sim stationary gyrons. Instead of the 6 or 10 twirlers shown forming that ring, however, many more are envisioned in reality. As one moves away from the ring in any direction, the VEGs have increasingly greater spin rates, and progressively changing average orientations.

F. "Breathing" VEGs. This constitutes a "larger sail" solution to "the motorboat problem" (hinted at in Part D; and see below). Each gyron—in this case with CW spin—precesses many times each orbit, as indicated by the 3-position composite shown at each orbit location. Each VEG is prone to gradual increases in its natural precession angle as it surfs the radially inflowing aether wind (see Figure 1C). By the time it reaches the southern hemisphere, it presents a much greater average cross-section to that wind than it did while in the northern hemisphere, helping to explain how vortices may absorb more momentum from the south, allowing them to remain stationary as they eject high speed GGs northward. Precession angles are greatly exaggerated for purpose of illustration.

Figure 3

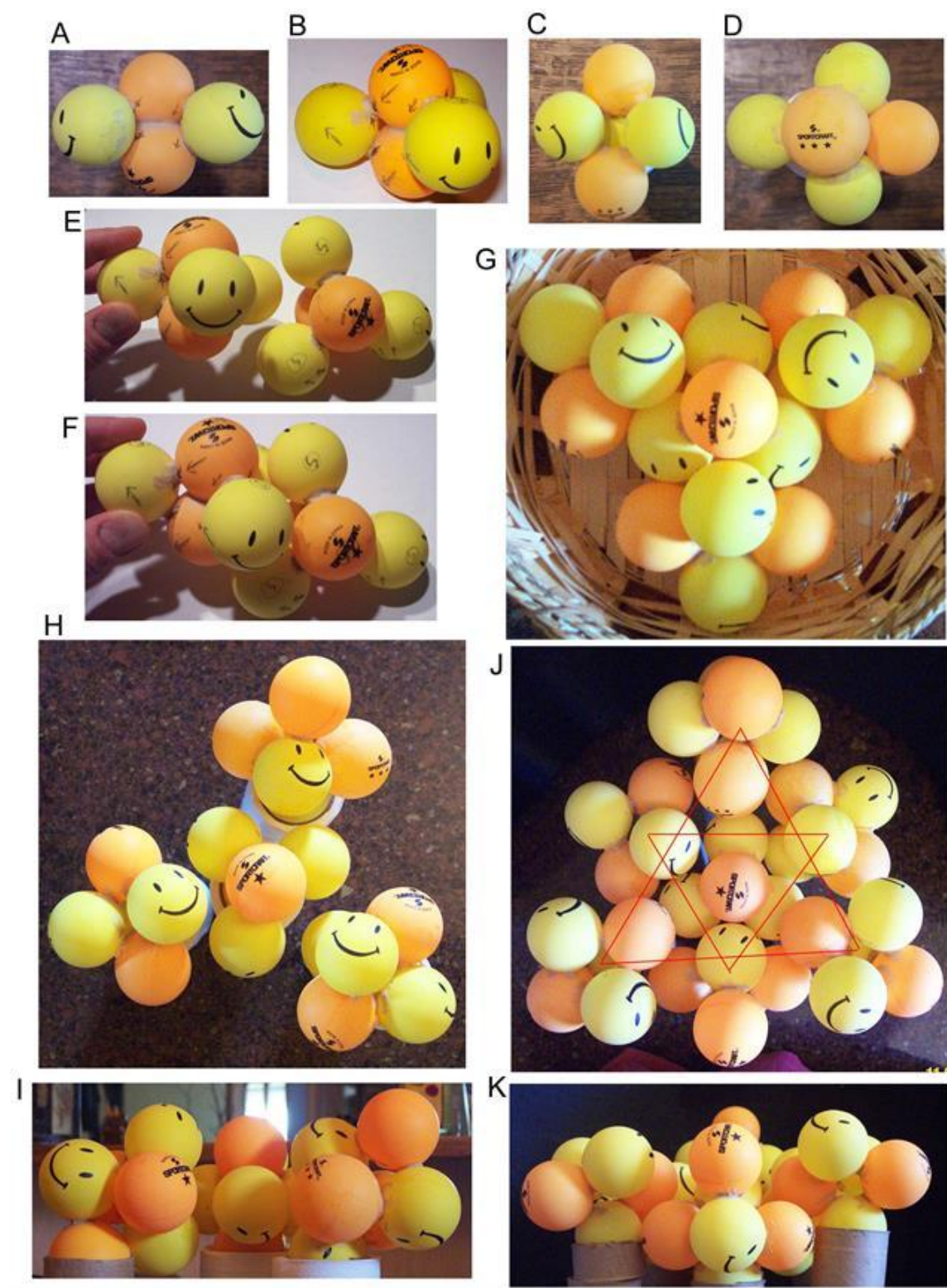


Fig. 3. Possible nucleon and nuclear structures

A. Side view of the proposed proton, with partly fused electrons (orange colored) at top and bottom, and two of the three positrons (yellow, with smiley “positive” faces) visible at right and left. The two electrons are lined up north-to-south, with a joint Z axis that coincides with the axis of the entire structure, providing a much longer and stronger funnel for ejecting high-speed, finely tuned GGs. Note: in order to explain some types of quantum non-locality, it may be necessary to have the positrons’ Z axes lined up opposite to that of the dual electron core, so that two distantly separated nucleons (or vacuum “virtual nucleons”) could each provide orientation stabilizing GG input to the other.

B. Alternate view of A, in which all three positrons can be seen.

C. Proton with unfused electrons, and a subsequently much longer joint Z axis.

D. Neutron, consisting of a proton as in C, viewed from above (looking down the Z axis), but with an additional electron attached, at the right. The three positrons and three electrons form two perpendicular triangles.

E. Two protons (with partially fused electrons) approaching one another, to show the alignment of positrons with electrons that produces the electrostatic shielding that partially accounts for the strong nuclear force’s attractive component, i.e., it helps explain why the protons do not move apart under their mutual electrostatic repulsion (assuming such even exists at this very short distance).

F. The same two protons as in E, now brought fully together in their closest-packed nuclear arrangement. The Z axes, defined by the electrons, are perpendicular.

G. Four protons together, illustrating the beautiful 3-fold symmetry of a 4-nucleon nucleus. The Z axes of the three peripheral protons are each perpendicular to that of the central one.

H. Helium-4 nucleus, top view, where the neutrons are at the top and lower right.

I. Helium-4 nucleus, side view from the right of panel H, showing that the left neutron’s electron (lower right in panel H) is at the bottom of the plane, whereas the rightmost neutron’s extra electron is on top of the plane. It may be appreciated from the side view that positrons stick out a bit along the top and bottom plane, where the extra electrons, rather than being bound to their respective neutrons, may move circularly in the plane of the nucleus, in a perfectly symmetrical arrangement. Both here and in Part K, the bottom halves of some of the electrons and positrons at the bottom are hidden by the cardboard tubes on which the nucleons are positioned.

J. Lithium-7 nucleus, top view. Three additional nucleons have been added to the three open spaces of the helium-4 nucleus. In this case, the three added nucleons have their electron axes (or planes, for the neutrons) perpendicular and radial to the central proton, rather than tangential as the other three. The 3 closest surrounding nucleon centers of helium-4 form the vertices of the small red triangle, while the additional 3, more distant nucleon centers of lithium-7 are indicated by the vertices of the larger red triangle.

K. Lithium-7 nucleus, side view. Its planar arrangement is still plainly visible.

Figure 4.

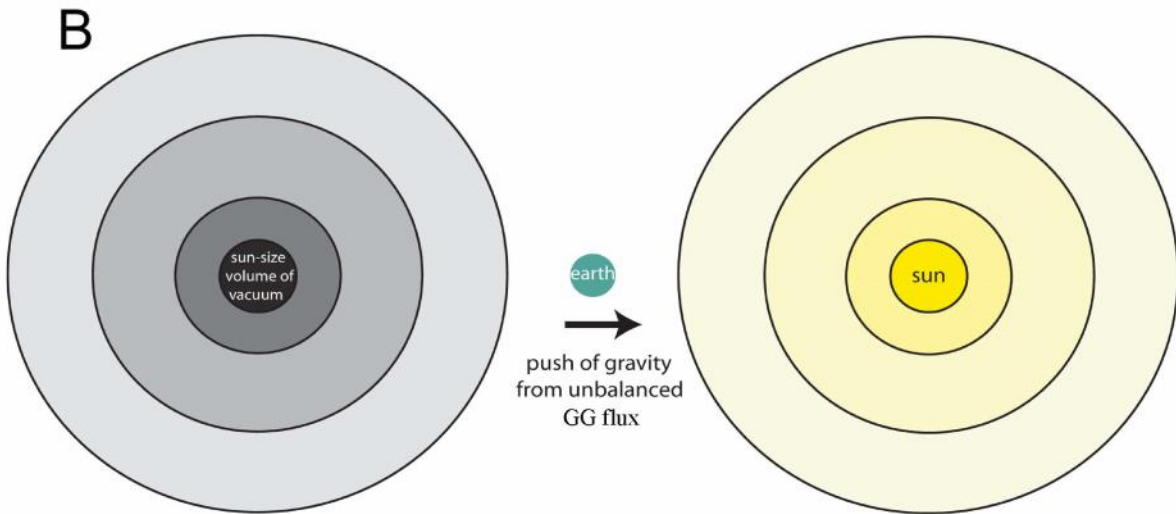
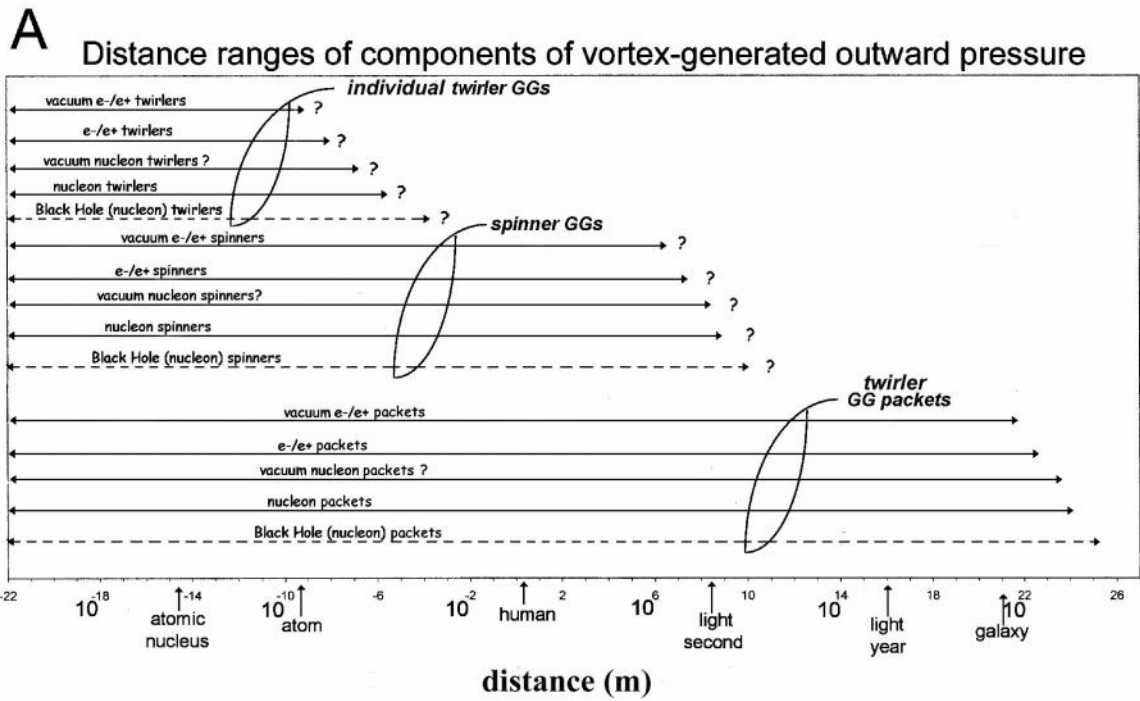


Fig. 4. Pressure differential gravity

A. A schematic illustration of the range of distances traveled by individual GGs and GG packets prior to experiencing catastrophic cascade collisions. The ejection of these various GGs from the corresponding vortices produces outward pressure from all such vortices. The question marks to the right of the individual twirler and spinner GG ranges indicate that I have little idea how far they can travel; the arrowhead endpoints are guesses, although their relative positions are deductions. Ones that happen to have their axis and translational vector perfectly aligned can travel vast distances without collision, unlike the components of ordinary gases. The individual GGs – both twirlers and spinners – may start out either as individuals or as parts of packets containing spinners, whose precessional motion quickly causes the packet to lose its tight packing and spread out, like a MIRV missile. Packets with only twirlers – shown in the bottom grouping – will retain their tight packing. That individual GGs can collide catastrophically after traveling essentially zero distance is indicated by the leftmost arrow tips resting at 10^{-22} m, an arbitrary cut-off used here for purpose of illustration. The arrowed lines showing black hole matter GG travel are dashed because of the highly speculative nature of their possibly exceeding the distances from ordinary matter vortices (see endnote 32).

B. The earth is pushed toward the sun by unbalanced gyron pressure. Because matter “tunes up” GGs (intercepts and re-emits them with lower cross-section) better than does a corresponding volume of vacuum, it represents a “negative pressure” on the aether, producing less outward pressure (relatively close by) than the less well-aligned GGs produced by the vacuum vortices. All reasonably large, super-molecular regions of space (i.e., not the sub-nuclear regions right next to vortex cores) are bombarded essentially equally from all sides by GGs, resulting in a constant agitation of the aether, i.e., a continual transfer of GG linear motion into vacuum gyron linear and twirling motion (and whose cycle is completed with the creation of new GGs by vortices in those small volumes of space). The earth, for example, is pushed toward the sun by the unbalanced nature of this pressure, as the sun is emitting GGs with less cross-sectional area than the corresponding sun-sized volume of vacuum on the opposite side of the earth. This treatment ignores possible secondary effects of the earth and sun on the surrounding vacuum.

C, D, and E. GG travel through the vacuum

Upper traces. Probability distribution histograms of the distances at which vacuum- vs. matter-generated GGs tend to collide catastrophically and return to the matrix rest frame. C differs from D and E in assuming an equal probability of catastrophic collision over every distance interval, while D2 assumes the operation of a “pathfinder” effect to clear the way for GGs as they exit their vortex. D3 and E additionally assume the existence of GG packets that can sustain multiple collisions spread out over large distances before the packet completely dissipates. D represents a slightly dispersed Poisson distribution, whereas E shows a very widely dispersed distribution, such as would occur if the vortices eject a wide array of various GGs (as hinted at in Part A).

Illustrated probabilities do not go to zero at zero distance because they are binned from zero to some arbitrary distance. Multimodal distributions are conceivable in D and E, with both a pathfinding effect and packet travel operating, but are not explored here.

Lower traces: the pressure exerted on the aether by the remaining emitted GGs, not including the $1/r^2$ radial dispersion, i.e., as if the gyrons were all traveling in one direction, as in a cylinder. The pressure is a complex function of GG speed (gradually decreasing only for GG packets) and reactivity (gradually increasing for packets), and thus follows the distribution curves faithfully only in C and D2 because individual GGs tend to react catastrophically soon upon their first collision. The pressure differential represents the strength of the gravitational “constant,” which thus changes with distance, although over the relatively small range of values we are accustomed to dealing with (solar system and smaller), it is essentially constant (especially in E, Distribution III). An unchanging pressure differential out to infinite distance would correspond to the current Newtonian and general relativity formulations, because we are not here factoring in the $1/r^2$ radial dispersion.

C represents an extreme case which cannot be obtained, if only because of an inevitable amount of pathfinding by previously ejected GGs. But GG packets are thought to be the predominant form in which GGs travel long distances, along with any individual GGs that may be following close behind. Depending upon the distributions and hence pressures of the vacuum and matter, the large variation illustrated by D2 may be obtained. The growing pressure on the galaxy scale, in the blue, attractive gravity zones in D2, D3, and E, may explain some of the evidence for “dark matter.” Note: the cross-over points for proportion of GGs reacted and for pressure need not correspond. Here, I am assuming that, on average, matter-emitted GGs have a greater speed, hence greater pressure for the same number of GGs. (The greater rate of GG generation by matter vortices has not been factored in, nor do these hand-drawn curves have exactly equal areas under the curve, as they should if they were correctly to represent total collision probability.)

F. Large-scale structure rationale for an initially sparse matter universe. The pressure differential from part D3 is reproduced on the left half of each panel, along with its mirror image on the right side. (The differentials of D2 or E would give the same general result.) Panel 1: masses A and B are separated by their zero point distance, i.e., that at which each’s gravitational tug has gone to zero (the pressure differential is zero at the “nose-tip of the blue dolphin”). A and B thus neither attract nor repel one another. Any closer and they would attract; further away and they would repel. (Note: for the presentation of this concept, the galaxy-size masses may reasonably be treated as point particles.) Panel 2: A and B repel, being in each other’s repulsive gravity zones, but all free spinners in the region are within one or the other’s zone of attraction (but those within the exact central plane would experience no net tug in either direction). This distance, a bit less than twice the zero point distance, is conjectured to be ~300 MLY, the average size of the

void space between galactic filaments/walls. Panel 3: A and B are situated at twice their zero point distance, and still repel one another (the red regions have not completely disappeared yet); any greater separation may result in new matter forming in between (as in Panel 4). The midway point here is a site of new vortex generation, as gravitational flows exist on either side, and also perhaps a site of low free spinner concentration for the same reason, assuming these weak gravitational flows are not overwhelmed by vortex-assisted diffusion of free spinners. Panel 4: A and B no longer exert any direct gravitational effect on each other, but *de novo* matter may form in the middle (labeled AB'), assuming the free spinner concentration there reaches a high enough level, due to repulsive gravity sweeping all the free spinners in the void space toward that central region. Panel 5: As in Panel 4, new matter may also form at this greater separation of galactic masses A and B. If it does, it would have converted itself to the situation shown in Panel 2. Panel 6: At this great separation, the repulsive gravity from A and B may be too weak, relative to vortex-assisted diffusion, to concentrate free spinners in the middle sufficiently to generate new matter. If new matter does manage to form, then even though the resulting situation would look, superficially, like something midway between the situations in Panels 3 and 4, the two resulting voids regions (between A and AB', and AB' and B) may have already been swept relatively clean of their free spinners, and no additional matter would form. This may help explain the large variability in the size of observed void spaces.

Supplementary Materials

I. Rough calculation of average gyron kinetics, based on an equation by Clausius

This calculation ignores the existence of the omnidirectional GG flux, and is an attempt to estimate the mean free path and average collision rate if all gyrons were twirlers with RMS speed c in a structureless gas. (Incidentally, a twirler with tip speed of c would be twirling at $6 \cdot 10^{42}$ Hz.) It is based upon Samuel Tolver Preston's (p.78 of ref. 16) statement of Clausius's equation, that the ratio of mean free path to "effective radius" is in the same proportion as the volume of space to (ether, or in this case, gyron) particle volume. Clausius derived his formula for spherical particles, which I'm trying to adapt here to thin cylinders.

The volume of space per gyron, assuming Meno's gyron density of 10^{96} per cubic meter, is 10^{-96} m^3 .

Assuming that a gyron, with length α and a very narrow waist region, has about half the volume of a cylinder whose diameter D equals that at the gyron's hip/shoulder region (using Meno's dimensions, where $D = \alpha/331$), the volume would be half of the length times the area, or $\frac{1}{2} \alpha \pi r^2$.

$$\begin{aligned} \text{Gyron volume} &\cong \frac{1}{2} [((1.616 \cdot 10^{-35} \text{ m})/331)^2] 1.616 \cdot 10^{-35} \text{ m} \\ &= \frac{1}{2} (4.22 \cdot 10^{-105} \text{ m}^3)/109,561 \\ &= 6.05 \cdot 10^{-110} \text{ m}^3 \end{aligned}$$

If the "effective radius" is $\frac{1}{4} \alpha (= 0.404 \cdot 10^{-35} \text{ m})$ – an educated guess – then

$$\begin{aligned} \text{mean free path} &= [(\text{space volume})/(\text{gyron volume})] * (\text{effective radius}) \\ &= [(10^{-96} \text{ m}^3)/(6.05 \cdot 10^{-110} \text{ m}^3)] * (0.404 \cdot 10^{-35} \text{ m}) \\ &= 6.68 \cdot 10^{-23} \text{ m} \\ &\cong 10^{-22} \text{ m} \end{aligned}$$

Assuming with Meno that the average gyron moves at about the speed of light, the number of collisions per second for the average gyron must be equal to the distance traveled per second divided by the distance traveled per collision (i.e., mean free path):

$$\text{Collisions per second} = (3 \cdot 10^8 \text{ m/s})/(6.68 \cdot 10^{-23} \text{ m}) = 4.5 \cdot 10^{30}/\text{s}.$$

However, for super-skinny gyrons with the much smaller width of $10^{-18} \alpha$ (rather than $\alpha/331$), similar calculations yield a mean free path of $\sim 7 \cdot 10^8 \text{ m}$, and ~ 0.5 collisions per second. This seems to give too much weight to the great reduction in gyron volume, and does not pay nearly

enough attention to the undiminished length, yielding what seems to be a much too large mean free path, and much too small a collision rate, especially given the results of section II, below. Probably more accurate, given that the gyrons would, on average (given an equipartition of energy between linear and twirling motion) twirl at a rate of $\sim 4 * 10^{42}$ Hz, would be to assume spheres of $r = \alpha/2$ so as to attempt initially to apply the Clausius equation exactly, and then scale the mean free path and collision rate by the projection of a unit length onto the X axis, that's tilted 45° along both the Y and Z axes (i.e., reduced by a factor of $0.707^2 = 0.5$). Proceeding essentially as above, this would yield, for mean free path, $\sim 4.6 * 10^{-28}$ m, and $6.6 * 10^{35}$ collisions per second.

II. Mean distance traveled by GGs

Based on Meno's proposed dimensions for the gyrons, one can calculate that the mean free path for a GG would be no more than $3.6 * 10^{-24}$ m, as follows.

Let's assume that a GG is a point traveling through a series of cubes, each of volume 10^{-96} m³, and each containing (on average) one gyron. We shall ask how many cubes, on average, will a GG pass through before colliding? Alternatively, we may ask how many cubes will it take for half of the cross-sectional area to be covered by the resident gyrons? The cross-sectional area of each cube is $(10^{-32} \text{ m})^2 = 10^{-64}$ m²; our GG, and each cube's gyron, must lie within that area. The area occupied by each gyron, on average, will be their maximal area diminished by the amount of average tilt they have, which I assume to be 45° in both the Y and Z dimensions (i.e., halfway between 0° and 90°). This will yield an effective length of $(\cos 45^\circ)^2 \alpha = 0.707^2 * \alpha = 0.5 \alpha$, where α = the Planck length ($1.616 * 10^{-35}$ m), i.e., Meno's proposed gyron length. Assume also that the average gyron width is half their maximal width, i.e., that at their hips and shoulders. For Meno, this would be $\alpha / 662$, giving a cross-sectional area for an average gyron of $(1.616 * 10^{-35} \text{ m}) * (0.5 * 1.616 / 662 * 10^{-35} \text{ m}) = 2.0 * 10^{-73}$ m². (For the super-skinny gyron of section I above, the cross-sectional area is $\sim 1.3 * 10^{-88}$ m².)

This area, divided by that of the cross-sectional area of each cube, gives the probability that our point-like GG will collide with the gyron whose volume of space (cube) it is passing through; $2.8 * 10^{-73} \text{ m}^2 / 10^{-64} \text{ m}^2 = 2.8 * 10^{-9}$. (For the super-skinny gyrons – see section I above – the value is $\sim 1.3 * 10^{-24}$.) Given a factor of two difference for resident gyron overlap, this means it'd travel through only $\sim 2 / (2.8 * 10^{-9})$ such cubes before colliding, which corresponds to a distance of $10^{-32} \text{ m} / (2.8 * 10^{-9}) = 7.2 * 10^{-24}$ m. (For super-skinny gyrons, $\sim 1.6 * 10^{-8}$ m.) This is two orders of magnitude shorter than the first "guesstimate" for the mean free path derived in section I above for ordinary gyrons using the Clausius equation. But, it is 4 orders of magnitude longer than the final guesstimate, suggesting that the latter is more accurate than the former. Since our GG is a

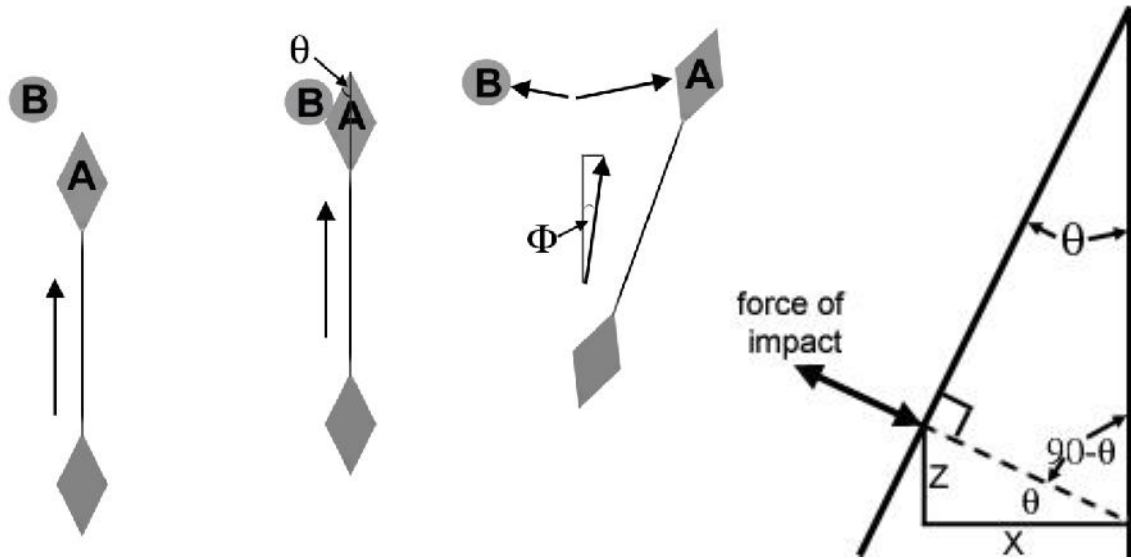
bit wider than a point, this actually represents a slightly larger mean free path than would actually obtain (although the approximation gets better as we make the width smaller.)

And so, in order to have our perfectly aligned GGs travel an average of 50,000 LY before colliding, if we want to keep their length the same, we'd have to postulate their width to be many orders of magnitude smaller than Meno's, so that the volume of space they occupy (and cross-sectional area they present to our GG) is correspondingly smaller. One LY = $0.946 * 10^{16}$ m, so our gyrons would have to be skinnier by a factor of $(50,000 * 0.946 * 10^{16} \text{m}) / (3.6 * 10^{-24} \text{m}) = 1.314 * 10^{44}$! (Versus the factor of 10^{18} for our super-skinny gyron calculations above and in section I.) And, in order to travel an average of 150 million LY, they'd have to be another $3 * 10^3$ skinnier, or $3.94 * 10^{47}$ fold skinnier than Meno's version. (Such an ultra-skinny gyron, if as long as the earth-moon distance, would still be 10^{15} -fold skinnier than a proton's diameter.)

Two complicating factors that can help produce the GG distance profile curves in Figure 4D and E are as follows:

- 1) a "pathfinder" effect, whereby previous GGs ejected from the same matter vortex "clear the trail" for subsequent GGs (at least for much of the initial distance, even though the material vortex changes its direction). For a vortex whose axis rotates at 1 Hz, to have successively ejected GGs be one gyron width (Meno's) apart at a distance of 1 meter would require an emission rate of 10^{38} /sec, and at a distance of 100 million light years, 10^{62} /sec. Such pathfinders could be mostly arrow-mode twirlers, rather than the possibly rare spinners. (I tend to not favor this operating over long distances, however, as it would seem then to leave little room for vortex structure anywhere, even if the "tunnels" are skinny and exist only briefly – although, again, one can argue that it's only a matter of degree, i.e., that the tunnels are "ultra-skinny," and thus may take up only tiny volumes for very brief instants.)
- 2) GGs may largely consist of unfathomably skinny twirlers traveling in tightly packed groups, termed GG packets, as described in the legends of Figure 1F, Figure 4A, and elsewhere in the text.

III. Calculation of angle of travel after a contact on a perfectly tuned GG's face



For this calculation, the gyron is assumed to be an idealized dumbbell consisting of two point masses at either end, connected by a massless rod. The gyron also is assumed to be spinning so rapidly that its precession angle after collision is negligible, and thus the reorientation of its angular momentum axis (greatly exaggerated in the drawing above) is also negligible. The face angle is theta (θ), and the deflection angle is phi (Φ). The situation is the same as those shown in Figure 1D and E, where gyron A is moving up, in the +Z direction, and contacts perpendicular, stationary (or relatively so) gyron B at the latter's midsection, i.e., at its center of mass. After the collision gyron A begins moving slightly to the right (+X direction) while gyron B begins moving to the left with half as much X velocity as A's top half, and their centers of mass move along x at equal and opposite speeds. For a brief instant immediately after contact, as the top half of A moves to the right at double the center of mass speed, the bottom half is stationary, and this situation reoccurs with every complete precession. (For gyrons with mass in the connecting rod, and in ones having non-point masses at the ends, the bottom half of A will move left to some extent toward B's position, possibly resulting in a double hit, which will serve only to increase A's deflection angle.)

Mass of an entire gyron = m , mass of top half of A = $m/2$, initial velocity of A = V_1 (all in +Z direction), initial velocity of B=0, final velocity of A in Z direction = $V_1(z)'$, X direction = $V_1(x)'$, final velocity of B in Z direction = $V_2(z)'$, final velocity of B in X direction = $V_2(x)'$.
Initial momentum = $m V_1$, initial kinetic energy (K.E.)= $\frac{1}{2} m V_1^2$

Looking at the illustration of gyron A's tip and the force of impact angle, we have $\tan \theta = z/x$, and essentially all of the mass of A behind the point of impact (exerting essentially zero torque on A, and exactly zero for point mass tips). X represents A's initial velocity (all in the +Z

direction), and Z represents the component of the impact force along the Z axis, and the proportion of Z-axis velocity transferred from A to B. (For example, if θ were zero, a frictionless contact on A's side could not slow its Z velocity at all, whereas if θ were 90° , such as directly on A's top point, or if A had a flat head, i.e., like a collision between two billiard balls hitting head on, all of A's motion would be transferred to B, and A would become motionless.)

If $\theta = 1^\circ$, we have $\tan 1^\circ = z/x = V_2(z)' / V_1 = 0.017455$; $V_2(z)' = 0.017455V_1$

$$mV_1 = m V_1(z)' + m V_2(z)'$$

$$V_1(z)' = V_1 - V_2(z)' = (1 - 0.017455)V_1 = 0.982545V_1$$

$$\text{K.E.}_{1Z}' = \frac{1}{2} m (0.982545V_1)^2 = 0.9654 \frac{1}{2} mV_1^2$$

$$\text{K.E.}_{2Z}' = \frac{1}{2} m (0.017455V_1)^2 = 0.0003045865 \frac{1}{2} mV_1^2$$

For momentum along the X axis, we have,

$$p_{1x}' = -p_{2x}' = mV_{2x}'; |V_{2x}'| = V_{1x}' = \frac{1}{2} V_{1(\text{tip})x}'$$

$$p_{1x}' = -\frac{1}{2} m V_{1(\text{tip})x}'$$

We're trying to extract A's x-axis motion from the equations describing total energy and momentum. Our simplifying assumption about A's mass being concentrated in two points at either end allows us to substitute the momentum and energy of A's tip immediately after contact for that of the entire gyron, and it also gave us the motion of A's center of mass. In this way we are able to account for the angular, twirling/precessing energy of A strictly in terms of the initial linear motion of A's top half. From here, it's just a matter of plugging in the numbers.

$$\text{K.E.}_{2x}' = \frac{1}{2} m (V_{1(\text{tip})x}'/2)^2 = \frac{1}{2} * \frac{1}{4} m V_{1(\text{tip})x}'^2 = m/8 V_{1(\text{tip})x}'^2$$

$$\text{K.E.}_{1x}' = \frac{1}{2} m/2 V_{1(\text{tip})x}'^2 = \frac{1}{4} m V_{1(\text{tip})x}'^2$$

(So, even though the top half of A has only half the mass of B, because energy goes as the square of speed and B moves half the speed of A's top half, A after the collision has twice the x-axis energy of B.)

Going back to the full energy equation, we have

$$\frac{1}{2} m V_1^2 = \frac{1}{2} m(V_{2z}'^2 + V_{2x}'^2) + \frac{1}{2} m V_{1Z}'^2 + \frac{1}{2} m/2 V_{1(\text{tip})x}'^2$$

Factoring out $\frac{1}{2} m$ and substituting terms, we have

$$V_1^2 = (0.017455V_1)^2 + V_{2x}'^2 + (0.982545V_1)^2 + \frac{1}{2} (-2 V_{2x}')^2$$

$$= 0.00030468V_1^2 + 3V_{2x}'^2 + 0.96539455V_1^2$$

$$= 0.9657V_1^2 + 3V_{2x}'^2$$

Solving for A's center-of-mass x-axis velocity,

$$V_{1(\text{center of mass})x}' = V_{2x}' = (0.03430077V_1^2/3)^{1/2} = (0.01143359V_1^2)^{1/2} \cong 0.107V_1$$

Thus, irrespective of how fast GG A spins, and no matter how small the precession angle resulting from the impact, A will assume a sideways speed more than one tenth its original Z-axis speed (which is itself reduced less than 2% in the case of a 1° face angle). This sideways motion of its center of mass will yield a deflection angle Φ , determined as follows (see figure showing Φ):

$$\tan \Phi = 0.106928/0.982545$$

$$\Phi = 6.21^\circ$$

Note that this is more than 6 times that of the face angle.

For a face angle of 0.1° and proceeding as before, we find that $\Phi = 1.955^\circ$, or almost 20 times the face angle. And for a face angle of 0.01°, we have $\Phi = 0.618^\circ$, almost 62 times the face angle. This is because the slighter and slighter decreases in A's z-axis motion produced by smaller and smaller face angles come at increasingly higher ranges of A's z-axis velocity, yielding proportionally more x-axis motion in return because of energy's variation with the square of velocity.

Thus, one finds that, at small face angles, for every 10-fold decrease in face angle, one decreases the deflection angle only by about a factor of 3. And no matter how small one imagines the face angle to be, in an attempt to have collisions be as undisruptive as possible, the resulting sideways deflection of the GG will make its cross-section much greater than that of just the face, opening up the entire length of the GG to collision with relatively stationary gyrons.

For a GG with ultra-fast spin, such that its precession angle and tilt away from the z-axis are so small as to be negligible, subsequent collisions, occurring at greater angles than the initial face angle collision and anywhere along the full length of the GG, will generally result in greater loss of energy, and greater sideways motion in the opposite direction, as illustrated in Figure 1G.